

Study of $e^+e^- \rightarrow \omega\chi_{cJ}$ at Center of Mass Energies
from 4.21 to 4.42 GeV

Yumo Su

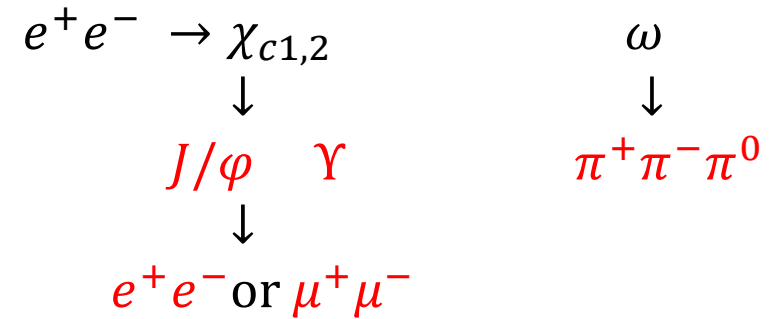
June. 9th ,2017

Motivation

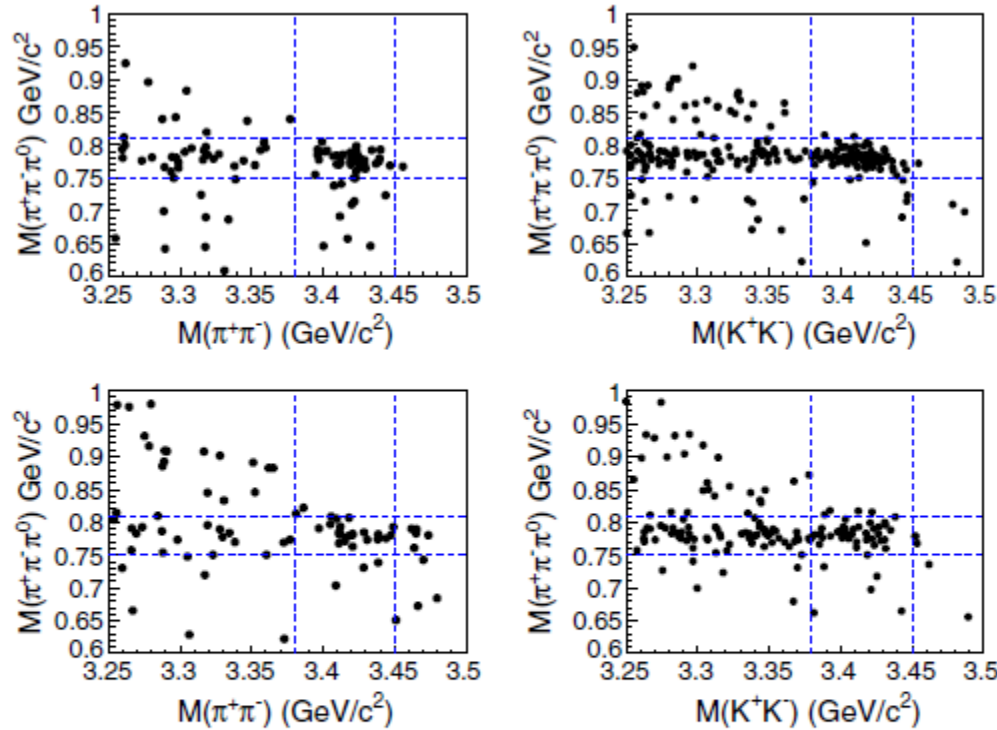
- Contrary to the hidden charm final states, the $Y(4260)$ were found to have small coupling to open charm decay modes, as well as to light hadron final states.
- Searches for new decay modes and measuring the line shape may provide information that is useful for understanding the nature of the $Y(4260)$

Reconstruction

A candidate event must have four tracks with zero net charge and at least one π^0 candidate; for the $e^+e^- \rightarrow \omega\chi_{c1,2}$ channels, an additional photon is required.



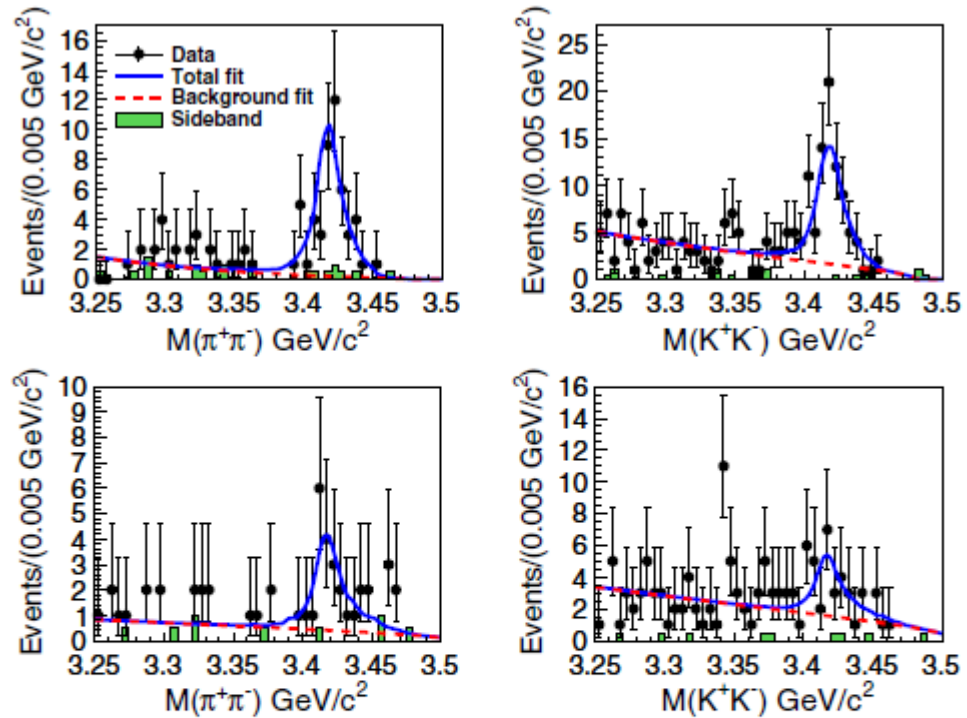
Some distributions of observable quantity in data



The main sources of background after event selection are found to be $e^+e^- \rightarrow \omega\pi^+\pi^-(\omega K^+K^-)$, where the $\pi^+\pi^-(K^+K^-)$ are not from χ_{c0} decays. The scatter plots of the invariant mass of $\pi^+\pi^-\pi^0$ versus that of $\pi^+\pi^-$ or K^+K^- for data at $\sqrt{s} = 4.23$ and 4.26 GeV are shown in Fig. 1. Clear accumulations of events are seen around the intersections of the ω and χ_{c0} regions, which indicate $\omega\chi_{c0}$ signals. Signal candidates are required to be in the ω signal region $[0.75, 0.81]$ GeV/c², The ω sideband is taken as $[0.60, 0.72]$ GeV/c² to estimate the nonresonant background.

FIG. 1 (color online). Scatter plots of the $\pi^+\pi^-\pi^0$ invariant mass versus the $\pi^+\pi^-$ (left) and K^+K^- (right) invariant mass at $\sqrt{s} = 4.23$ GeV (top) and 4.26 GeV (bottom). The dashed lines denote the ω and χ_{c0} signal regions.

Fit



The signal is described with a shape determined from the simulated signal Monte Carlo sample. The background is described with an ARGUS function.

FIG. 2 (color online). Fit to the invariant mass distributions $M(\pi^+\pi^-)$ (left) and $M(K^+K^-)$ (right) after requiring $M(\pi^+\pi^-\pi^0)$ in the ω signal region at $\sqrt{s} = 4.23$ GeV (top) and 4.26 GeV (bottom). Points with error bars are data, the solid curves are the fit results, the dashed lines indicate the background, and the shaded histograms show the normalized ω sideband events.

Results

TABLE I. The results on $e^+e^- \rightarrow \omega\chi_{c0}$. Shown in the table are the integrated luminosity \mathcal{L} , the product of the radiative correction factor, the branching fraction and efficiency $\mathcal{D} = (1 + \delta^r)[\epsilon_\pi\mathcal{B}(\chi_{c0} \rightarrow \pi^+\pi^-) + \epsilon_K\mathcal{B}(\chi_{c0} \rightarrow K^+K^-)]$, the number of observed events N^{obs} (the numbers of background are subtracted at $\sqrt{s} = 4.23$ and 4.26 GeV), the number of estimated background N^{bkg} , the vacuum polarization factor $(1 + \delta^v)$, the Born cross section σ^B , and the upper limit (at the 90% C.L.) on the Born cross section σ_{UL}^B at each energy point. The first uncertainty of the Born cross section is statistical, and the second is systematic. The three center dots mean not applicable.

| \sqrt{s} (GeV) | $\mathcal{L}(\text{pb}^{-1})$ | $\mathcal{D}(\times 10^{-3})$ | N^{obs} | N^{bkg} | $1 + \delta^v$ | σ^B (pb) | σ_{UL}^B (pb) |
|------------------|-------------------------------|-------------------------------|------------------|------------------|----------------|---------------------------------|-----------------------------|
| 4.21 | 54.6 | 1.99 | 7 | 5.0 ± 2.8 | 1.057 | $20.2^{+46.3}_{-37.7} \pm 3.3$ | <90 |
| 4.22 | 54.1 | 2.12 | 7 | 4.3 ± 2.1 | 1.057 | $25.1^{+39.4}_{-30.4} \pm 2.0$ | <81 |
| 4.23 | 1047.3 | 2.29 | 125.3 ± 13.5 | ... | 1.056 | $55.4 \pm 6.0 \pm 5.9$ | ... |
| 4.245 | 55.6 | 2.44 | 6 | 4.0 ± 1.5 | 1.056 | $16.3^{+30.8}_{-22.3} \pm 1.5$ | <60 |
| 4.26 | 826.7 | 2.50 | 45.5 ± 10.2 | ... | 1.054 | $23.7 \pm 5.3 \pm 3.5$ | ... |
| 4.31 | 44.9 | 2.56 | 5 | 2.2 ± 1.6 | 1.053 | $26.2^{+34.9}_{-25.1} \pm 2.2$ | <76 |
| 4.36 | 539.8 | 2.62 | 29 | 32.4 ± 4.7 | 1.051 | $-2.6^{+6.1}_{-5.4} \pm 0.27$ | <6 |
| 4.39 | 55.2 | 2.57 | 2 | 0.6 ± 0.7 | 1.051 | $10.4^{+20.7}_{-11.2} \pm 0.7$ | <37 |
| 4.42 | 44.7 | 2.46 | 0 | 1.4 ± 1.5 | 1.053 | $-13.6^{+18.5}_{-14.7} \pm 1.3$ | <15 |

For the process $e^+e^- \rightarrow \omega\chi_{c1,2}$, no obvious signals are observed at $\sqrt{s} = 4.31, 4.36, 4.39$ and 4.42 GeV.

TABLE II. The results on $e^+e^- \rightarrow \omega\chi_{c1,2}$. Listed in the table are the product of the radiative correction factor, the branching fraction and efficiency $\mathcal{D} = (1 + \delta^r)(\epsilon_e\mathcal{B}(J/\psi \rightarrow e^+e^-) + \epsilon_\mu\mathcal{B}[J/\psi \rightarrow \mu^+\mu^-])$, the number of the observed events N^{obs} , the number of backgrounds N^{bkg} in the sideband regions, and the upper limit (at the 90% C.L.) on the Born cross section σ_{UL}^B .

| Mode | \sqrt{s} (GeV) | $\mathcal{D}(\times 10^{-2})$ | N^{obs} | N^{bkg} | σ_{UL}^B (pb) |
|-------------------|------------------|-------------------------------|------------------|---------------------|-----------------------------|
| $\omega\chi_{c1}$ | 4.31 | 1.43 | 1 | $0.0_{-0.0}^{+1.2}$ | <18 |
| | 4.36 | 1.27 | 1 | $1.0_{-0.8}^{+2.3}$ | <0.9 |
| | 4.39 | 1.27 | 1 | $0.0_{-0.0}^{+1.2}$ | <17 |
| | 4.42 | 1.25 | 0 | $0.0_{-0.0}^{+1.2}$ | <11 |
| $\omega\chi_{c2}$ | 4.36 | 0.95 | 5 | $1.0_{-0.8}^{+2.3}$ | <11 |
| | 4.39 | 1.06 | 3 | $0.0_{-0.0}^{+1.2}$ | <64 |
| | 4.42 | 0.98 | 2 | $0.0_{-0.0}^{+1.2}$ | <61 |

Summary

The process $e^+e^- \rightarrow \omega\chi_{c0}$ is observed at $\sqrt{s} = 4.23$ and 4.26 GeV for the first time, and the Born cross sections are given. For other energy points, no significant signals are found.

The process $e^+e^- \rightarrow \omega\chi_{c1,2}$ channels are also sought for, but no significant signals are observed .

By examining the $\omega\chi_{c0}$ cross section as a function of center of mass energy, find that it is inconsistent with the line shape of the $Y(4260)$ observed in $e^+e^- \rightarrow \pi^+\pi^-J/\psi$. This suggests that the observed $\omega\chi_{c0}$ signals are unlikely to originate from the $Y(4260)$